Current Biology *18*, 1978–1985, December 23, 2008  DOI 10.1016/j.cub.2008.11.023

Report

# Extracellular Sugar Modifications Provide Instructive and Cell-Specific Information for Axon-Guidance Choices

**Hannes E. Bülow,[1,2,3,*] Nartono Tjoe,[3] Robert A. Townley,[1] Dominic Didiano,[3] Toin H. van Kuppevelt,[4] and Oliver Hobert[3]**

[1]Department of Genetics
[2]Dominick P. Purpura Department of Neuroscience
Albert Einstein College of Medicine
Bronx, NY 10461
USA
[3]Department of Biochemistry and Molecular Biophysics
Howard Hughes Medical Institute
Columbia University Medical Center
New York, NY 10032
USA
[4]Department of Biochemistry
Radboud University Nijmegen Medical Centre
Nijmegen Centre for Molecular Life Sciences (NCMLS)
6500 HB Nijmegen
The Netherlands

## Summary

**Heparan sulfates (HSs) are extraordinarily complex extracellular sugar molecules that are critical components of multiple signaling systems controlling neuronal development [1–3]. The molecular complexity of HSs arises through a series of specific modifications, including sulfations of sugar residues and epimerizations of their glucuronic acid moieties. The modifications are introduced nonuniformly along protein-attached HS polysaccharide chains by specific enzymes [4]. Genetic analysis has demonstrated the importance of specific HS-modification patterns for correct neuronal development [2, 3]. However, it remains unclear whether HS modifications provide a merely permissive substrate or whether they provide instructive patterning information during development. We show here with single-cell resolution that highly stereotyped motor axon projections in *C. elegans* depend on specific HS-modification patterns. By manipulating extracellular HS-modification patterns, we can cell specifically reroute axons, indicating that HS modifications are instructive. This axonal rerouting is dependent on the HS core protein *lon-2*/glypican and both the axon guidance cue *slt-1*/Slit and its receptor *eva-1*. These observations suggest that a changed sugar environment instructs *slt-1*/Slit-dependent signaling via *eva-1* to redirect axons. Our experiments provide genetic in vivo evidence for the "HS code" hypothesis which posits that specific combinations of HS modifications provide specific and instructive information to mediate the specificity of ligand/receptor interactions [3, 5, 6].**

## Results

### Distinct HS-Modification Patterns Are Required by Individual Ventral Cord Motor Neurons for Correct Axon Pathfinding

The DA and DB classes of motor neurons are embryonically generated motor neurons (eMNs) in the ventral nerve cord (VNC) of *C. elegans.* Individual DA and DB motor neurons make differential, completely invariant choices as to whether to extend circumferentially along the right or left side of the animal (Figures 1B–1D). This sidedness does not correlate with the membership of a motor neuron to a specific class (e.g., two DA neurons extend along the right side, and seven DA neurons extend to the left side; Table S1 available online), nor position along the a/p axis (Figure 1B; Table S1), lineage history (Table S1), or any other unique cellular landmark in their environment (Table S1). Intriguingly, there are no molecular markers that distinguish individual DA neurons or individual DB neurons from one another (i.e., no genes are known that are expressed in DB2 but not DB3) and no genes have been reported that control the cell-type specificity of the projection patterns. To test whether individual DA/DB motor neurons require distinct HS modifications for correct development, we genetically removed three major HS-modifying enzymes, the C5-epimerase encoded by *hse-5,* the 6O-sulfotransferase encoded by *hst-6*, and the 2O-sulfotransferase, encoded by *hst-2* (Figures 1A and 1E). Because none of these enzymes have paralogs in *C. elegans,* we can assume that animals with null mutations in these genes completely lack C5-epimerization, 6O-sulfation, or 2O-sulfation [7]. Removal of C5-epimerization or 2O-sulfation each result in mild defects in the sidedness of motor axon projections [7]. These mild defects show cell-type specificity, with DA2, DB3, DB6, and DB7 being most affected by loss of 2O-sulfation (Figure 1E). Generation of double mutants as well as a triple mutant resulted in significantly enhanced mutant phenotypes, revealing cell-type-specific redundancies in the requirement of HS modifications for individual motor axons (Figure 1F). For example, the DA2, DB3, and DB6 motor neurons display significantly enhanced defects in the *hst-6 hst-2* and *hse-5*; *hst-6* double mutant combinations, indicating that *hst-6* function is redundant with both *hse-5* and *hst-2* in these motor neurons. However, in DA6 motor neurons, *hst-6* function is redundant with *hse-5* but not with *hst-2*, whereas, in DB5 motor neurons, *hst-6* is redundant with *hst-2* but not with *hse-5* (Figure 1F). The HS-modification enzymes *hst-6* and *hst-2*/*hse-5* appear to act in different tissues during neuronal development, with *hst-6* acting in neuronal tissues and *hse-5*/*hst-2* in hypodermal tissues [7]. Thus, the observation that *hst-6* and *hse-5*/*hst-2* serve redundant functions in some neurons may seem nonintuitive given their disparate sites of action. However, HS has been demonstrated to act cell nonautonomously in, for example, ectodermal/mesodermal interactions [8]. It is therefore conceivable that differentially modified HS on neuronal and hypodermal tissues cooperate in a redundant manner to control axon routing.

In contrast, the defects in *hse-5*; *hst-2* double mutants are no more severe than the defects in the most severe (*hst-2*) of the single mutants (Figure 1F). This last finding is consistent with analyses in other cellular contexts that demonstrate that *hse-5* and *hst-2* can genetically act in the same pathway [7]. Finally, no further enhancement is observed in the triple mutant combination compared to the *hst-6 hst-2* double null mutant (Figure 1F). We conclude that individual members of the same class of motor neurons (DA or DB) that make apparently

*Correspondence: hbuelow@aecom.yu.edu

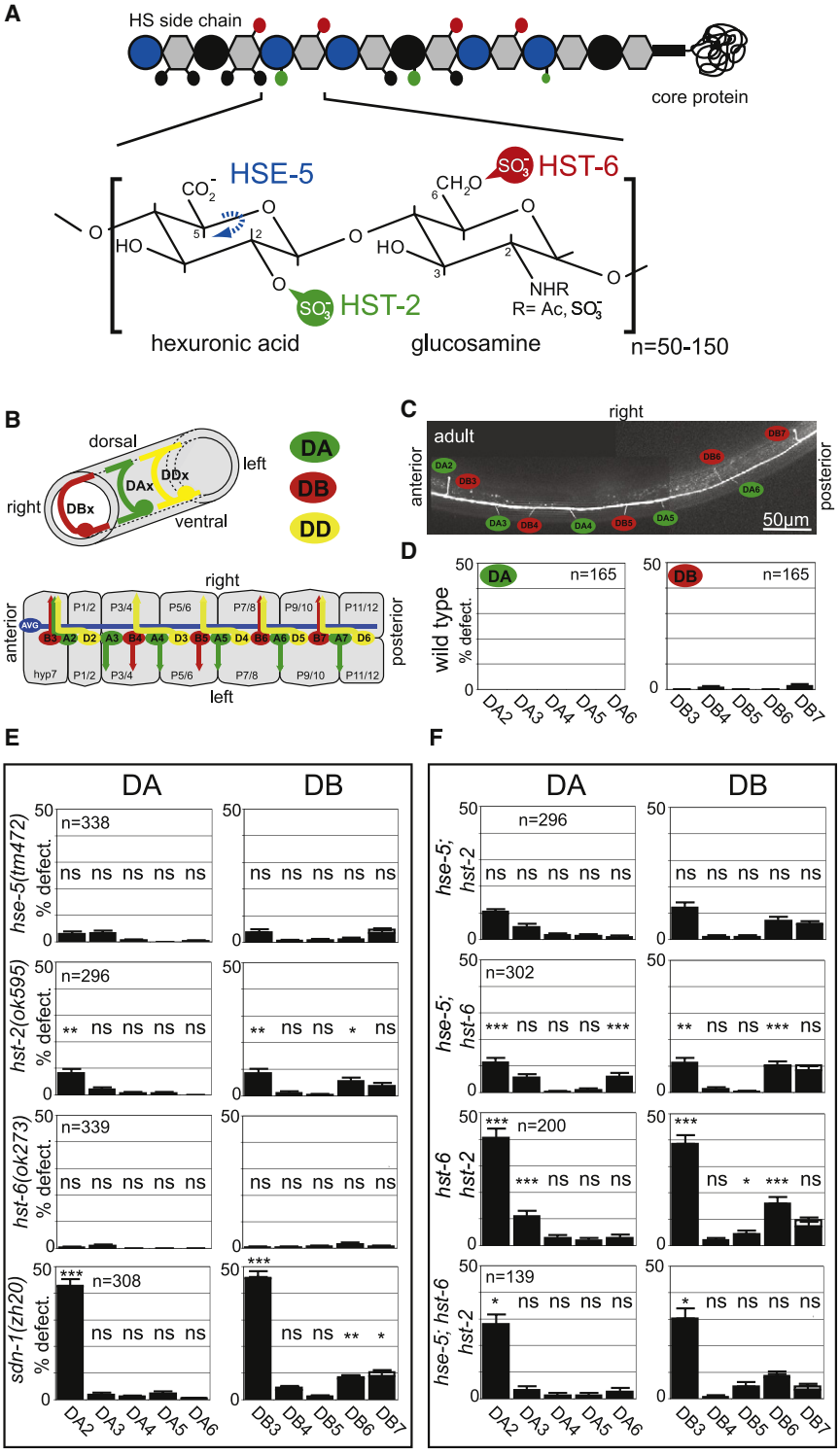


Figure 1. Individual DA/DB Motor Neurons Require Distinct Combinations of HS Modifications

(A) Heparan sulfate is a polymer composed of highly modified disaccharide repeats that is attached to a core protein. Shown is a characteristic HS disaccharide repeat unit consisting of a hexuronic acid (circle) and a glucosamine (hexagon) residue and enzymes that modify this structure. Large blue versus black circles indicate iduronic acid versus glucuronic acid, respectively. Small circles in black, green, and red indicate modifications as color coded in the disaccharide repeat. HSE-5, HS C5 epimerase; HST-X, HS XO-sulfotransferase (X = 2, 6).

(B) The top panel shows the circumferential axonal trajectory of exemplary DA-, DB-, and DD-type eMNs. eMNs are distinguished by their axonal projection patterns and by the neurotransmitter, which they express. The lower panel shows a schematic "open book" representation of the 2- to 3-fold embryonic stage when eMN axon outgrowth occurs, illustrating that individual DA, DB eMNs show a distinct sidedness of circumferential axonal growth. The eMN cell bodies shown here lie on top of the junctions between bilaterally symmetry P1/2, P3/4, P5/6, P7/8, P9/10, and P11/12 hypodermal cells. More anteriorly and posteriorly positioned eMNs are not shown (see Experimental Procedures). The only other axon that populates the VNC at that stage is the axon of the AVG pioneer neuron. See Table S1 for a systematic comparison of individual motor neuron class members.

(C) Visualizing the DA and DB motor axons with an *unc-129::gfp*-expressing transgene.

(D) The left/right asymmetric, circumferential DA, DB axon projection patterns are highly stereotyped. We focus our scoring on the DA2 to DA6 and DB3 to DB7 motor neurons because those express the *gfp* reporter transgene most reliably. "% defect." indicates percentage of animals with a defective sidedness of the respective DA or DB axon as indicated.

(E) Loss of HS modifications affect DA and DB axon choices in a cell-type-specific manner. All mutants used are null mutants [7, 31]. Single mutants were statistically compared to wild-type (see [D]); ns, not significantly different; *p < 0.05, **p < 0.005.

(F) Comparison of effects of single, double, and triple HS mutants on specific motor axons. Double mutants were statistically compared to the more severe of two respective single mutants; ns, not significantly different; *p < 0.05, **p < 0.005, ***p < 0.0005. The defects in both DA2 and DB3 are weakly statistically significant when comparing the triple *hse-5; hst-6 hst-2* mutant and the *sdn-1*/syndecan null mutant (p = 0.04 and 0.03, respectively). However, these differences are not significant between the *hst-6 hst-2* double mutant and either the *sdn-1*/syndecan mutant or the *hse-5; hst-6 hst-2* triple mutant, suggesting that the phenotype of the *sdn-1* and the *hse-5; hst-6 hst-2* triple mutant is very similar. Error bars denote the standard error of proportion. See Experimental Procedures for statistics.

identical guidance choices at the ventral midline of *C. elegans* are dependent on different combinations of HS modifications.

Removal of the HS core protein syndecan (*sdn-1*) recapitulates the defects observed in *hse-5; hst-6 hst-2* triple mutants, both in terms of penetrance and cell-type specificity (Figures 1E and 1F). In contrast, neither null mutations in the two *C. elegans* glypican HS core proteins (*gpn-1* and *lon-2*; [9, 10]) nor mutations in the secreted HS core proteins *unc-52* (perlecan; [11]) or *cle-1* (collagen XVIII; [12]) display significant defects in eMN left/right projection patterns (Figure S1A). These results suggest that the majority of HS that controls DA/DB motor axon choices may be attached to the syndecan core protein.

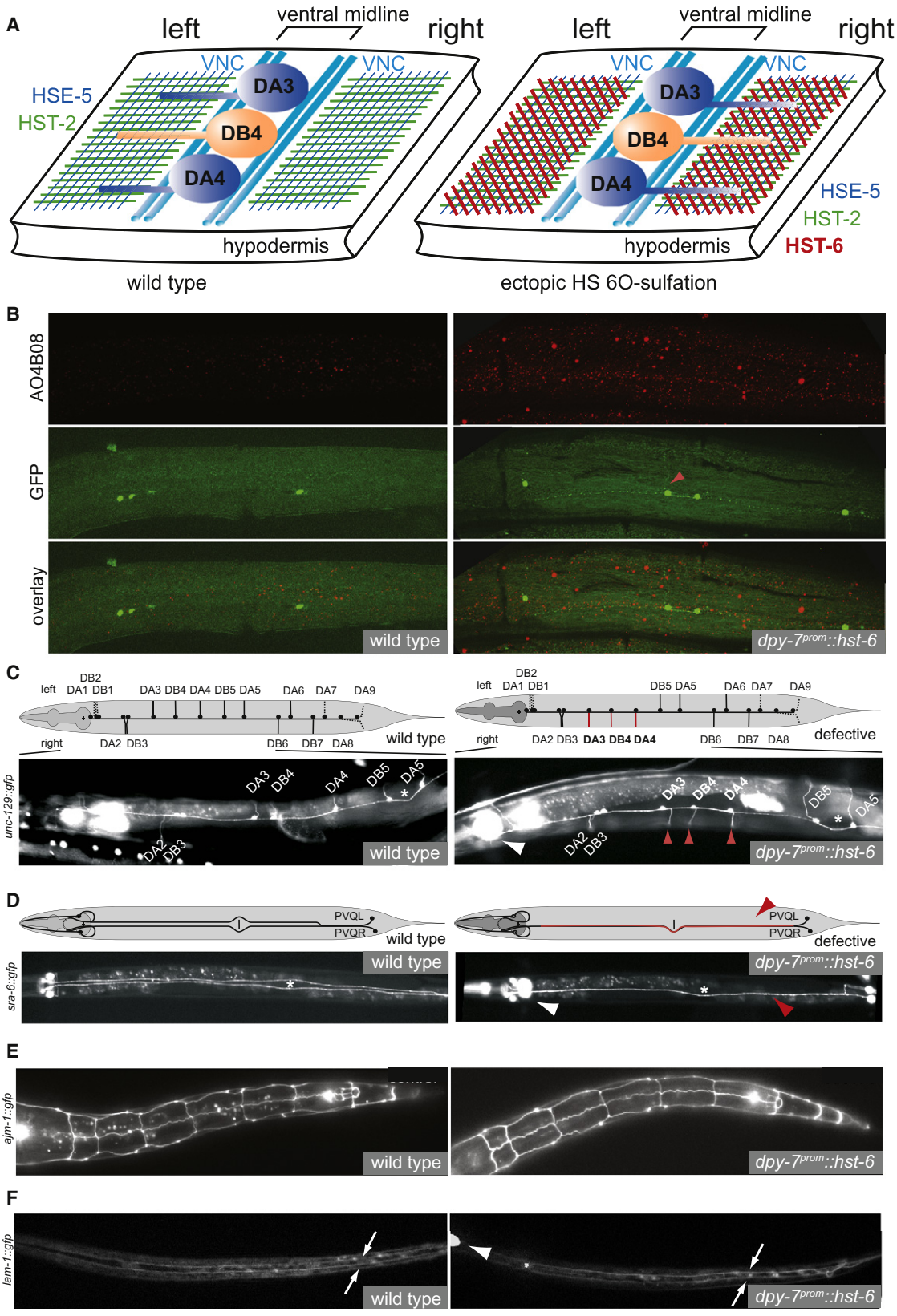


Figure 2. Manipulating HS-Modification Patterns Redirects Motor Axons

(A) Schematic view of the ventral cord with HS modifications in the hypodermis indicated by colored hatchings. Note that unlike in larvae, the embryonic midline, defined as a physical barrier between the left and right ventral fascicles, is not constituted by a hypodermal evagination but by motor neuron cell bodies [32].

### Manipulating HS-Modification Patterns Redirect Motor Axon Projections

Our present work with DA/DB motor neurons together with previous work shows that the function of HS requires their extensively modified polysaccharide chains (Figure 1A; reviewed in [3, 13]). However, it is unclear whether HS modifications constitute a merely permissive environment or whether they are sufficient to guide growing axons. The question of permissiveness versus instructiveness represents one of the key problems in the HS field [3, 13].

To address whether HS modifications are sufficient to guide axons, i.e., serve instructive functions, we manipulated HS-modification patterns by inducing ectopic 6O-sulfation in the hypodermal cells that underlie the DA/DB motor neurons (Figure 2A). The 6O-sulfotransferase *hst-6* does not appear to be expressed in hypodermal cells [7] (Figure 2A) and as shown above, DA/DB axon choices are unaffected by removal of *hst-6* alone (Figure 1E). To alter HS-modification patterns presented by hypodermal cells, we generated multiple transgenic *C. elegans* lines that aberrantly express *hst-6* in an otherwise wild-type background under control of the hypodermis-specific *dpy-7* promoter [14]. Worms expressing this construct show an altered status of HS-modification patterns. First, we detect novel staining patterns with an antibody that recognizes HS epitopes comprising specific oligosaccharides rather than individual modifications (Figure 2B) [15]. This antibody labels the anterior intestine and possibly some neurons and basement membranes in wild-type animals (not shown). However, increased staining is observed consistently in the hypodermis upon misexpression of *hst-6* in this tissue. This increased staining pattern is not observed in nontransgenic but otherwise isogenic controls (Figure 2B). And second, biochemical analyses of HS from transgenic worms expressing *hst-6* in the hypodermis display an increase of 6O-sulfated relative to 2O-sulfated HS disaccharides (Figure S2). Each transgenic line shows a significant number of animals in which the projections of individual DA and DB motor neurons are rerouted (Figures 2C and 3A; Figure S3). These defects are not the result of apparent changes in cell fate or structure of hypodermal cells misexpressing *hst-6* (Figure 2E), nor are they due to changes in eMN positioning in the VNC (data not shown). Moreover, we cannot detect obvious disruptions of the basement membranes surrounding eMNs and therefore consider it unlikely that ectopic *hst-6* expression grossly disrupts midline structures (Figure 2F).

The axonal misrouting defects we observe are the result of *hst-6* activity as the introduction of a premature stop codon into the *hst-6* expression construct abolishes its ability to induce axon misrouting (Figure 3A). Furthermore, no comparable misrouting defects can be observed upon *dpy-7*$^{prom}$-driven overexpression of the HS 2O-sulfotransferase *hst-2* (Figure 3A), which is normally expressed in both neuronal and hypodermal tissues [7]. These *hst-2* expressing transgenes are functional: First, the transgenes are able to effectively rescue neuronal *hst-2* loss-of-function phenotypes (Figure S4A); second, by using an antibody recognizing specific HS epitopes, we detect increased staining in transgenic, *hst-2*-overexpressing strains (Figure S4B); third, biochemical analyses of *hst-2*-overexpressing strains display increased 2O-sulfation relative to 6O-sulfation compared to wild-type (Figure S2). Together, our results argue that the effects of ectopic *hst-6* expression are due to the regiospecific addition of a sulfate moiety to the 6O-hydroxyl group of the glucosamine residue, rather than the unspecific addition of a negative charge.

Examining the axon choices of individual DA and DB motor axons, we find that the defects induced by ectopic 6O-sulfation are cell-type specific with all different transgenic lines displaying qualitatively similar misrouting patterns. Interestingly, there seems to be a graded response of DB neurons to misexpressed *hst-6*, with the more posterior neurons being more strongly affected (Figure 3C; Figure S3). In contrast, within the DA class of eMNs, only DA3 exhibits significant defects. Ectopic hypodermal 6O-sulfation also causes axon guidance defects in a selected number of other neurons in the nervous system. For example, axon midline guidance of the PVQ interneurons is affected (Figures 2D and 3B), whereas many neurons, such as touch neurons, amphid, phasmid, and RMEV neurons display no apparent defects (Table S2). Notably, PVQ interneurons are also affected by loss of endogenous, neuronally acting *hst-6* [7]. The addition of 6O-sulfation in the wrong location (hypodermis) can therefore have the same detrimental effect for an axon as not having 6O-sulfation in the correct place (neurons). Taken together, manipulating HS modifications in the hypodermis through addition of novel HS-modification patterns can redirect axonal projections of individual neurons.

### Ectopic 6O-Sulfation-Induced Motor Axon Misrouting Requires Slit/*slt-1* and Its Coreceptor *eva-1*

Most DA/DB motor neurons that respond to ectopic HS 6O-sulfation require *hst-6* also for normal development in the absence of *hst-2* function (compare Figures 1E, 1F, and 3C). The exception is DB7, suggesting that DB7 axonal projections are normally independent of 6O-sulfated HS. However, upon *hst-6* expression in the hypodermis, DB7 is misrouted, suggesting that DB7 can be positively instructed by ectopic 6O-sulfated

(B) Immunostaining with the AO4B08 HS-specific antibody [15] of transgenic animals, which ectopically express the HS-modification enzyme *hst-6* in the hypodermis (right; *otIs176*). Increased hypodermal staining observed in transgenic animals is not seen in isogenic controls, which do not ectopically express *hst-6* (left). Intestinal staining (not shown) serves as an internal staining control as does an unrelated synthetic antibody (MPB49), which shows no staining at all. Note that the antibody AO4B08 does not recognize individual HS modifications but rather an oligosaccharide, which requires the activities of both *hst-2* and *hst-6* [15]. Because only *hst-2* but not *hst-6* appears to be expressed in the hypodermis [7], the observed staining of the hypodermis after misexpression of *hst-6* in this tissue is consistent with the known specificities of AO4B08. Note the aberrant projection of DB6 in the *hst-6*-misexpressing line (red arrowhead).

(C) Axonal misrouting of DA/DB motor neurons in animals with ectopic *hst-6* expression in the hypodermis (right, *otEx1711*). Dashed lines indicate neurons that were not scored and affected neurons are in red. See Figure 3 and Figure S3 for quantification of defects.

(D) Midline crossover defects of PVQ interneurons in animals with ectopic *hst-6* expression in the hypodermis (right, *otEx1711*).

(E) Hypodermal cell fate as well as cell morphology, as visualized by normal AJM-1 expression and localization patterns, is not visibly affected by ectopic *hst-6* expression (right, *otIs176*).

(F) Basement membrane topology, as visualized by a *lam-1::gfp* reporter (kind gift of David Sherwood) [33], is not visibly affected by ectopic *hst-6* expression (right, *otIs176*). Arrows point to the basement membrane that ensheathes the ventral midline and which visually appears most concentrated on each side of the midline as a result of optical sectioning. Left panels represent wild-type controls in all cases. White arrowheads point to pharyngeal expression of *gfp* denoting the presence of the hypodermal *hst-6* misexpression array, and red arrowheads indicate axonal routing errors. All views are ventral aspects with anterior to the left.

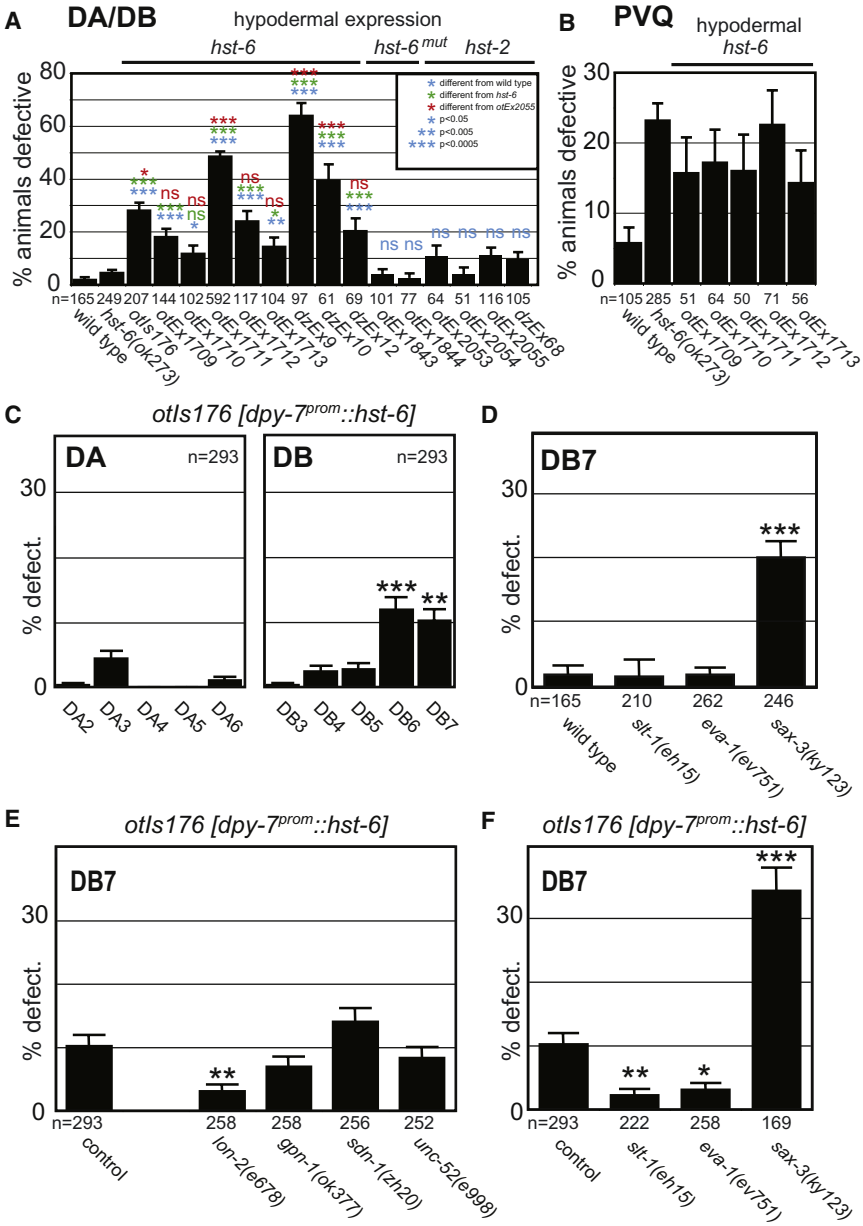


Figure 3. Genetic Analyses of *hst-6*-Dependent Axonal Misrouting Phenotypes

(A) Quantification of DA/DB motor neuron defects in different transgenic strains that express the indicated constructs from the hypodermal-specific *dpy-7* promoter. Shown is the percentage of animals with any number (≥1 per animal) of DA or DB axon sidedness defects.

(B) Quantification of midline crossover defects in PVQ interneurons in different transgenic strains that express *hst-6* from the hypodermal-specific *dpy-7* promoter.

(C) Effect of ectopic *hst-6* expression on individual DA and DB neurons. One representative line is shown here, five more extrachromosomal lines are shown in Figure S2B. Shown is the percentage of animals with defects in individual DA/DB motor axons projections as indicated.

(D) Defects in DB7 motor axon projection patterns in different mutants of the Slit/Robo signaling pathway as indicated. Shown is the percentage of animals with defects in DB7 motor axon projections.

(E) Effect of genetic removal of HS core proteins on projection errors in DB7 motor axons as a result of ectopic *hst-6* expression. Shown is the percentage of animals with defects in DB7 motor neuron projections. Statistic comparisons are made to the transgenic control. The projection pattern of DB7 in animals that misexpress *hst-6* in the hypodermis and are also mutant for *lon-2* is statistically indistinguishable from nontransgenic, wild-type animals.

(F) Effect of removal of genes in the Slit/Robo signaling pathway on projection errors in DB7 motor axons as a result of ectopic *hst-6* expression. Shown is the percentage of animals with defects in DB7 motor axon projections. Statistic comparisons are made to the transgenic control. The projection pattern of DB7 in animals that misexpress *hst-6* in the hypodermis and are also mutant for *slt-1* or *eva-1* is statistically indistinguishable from nontransgenic, wild-type animals. Error bars denote the standard error of proportion. Statistical significance is indicated by ns, not significantly different; *p < 0.05, **p < 0.005, ***p < 0.0005 in all panels.

HS. We therefore focus our genetic analyses here on the DB7 motor neuron.

We first asked which HS core protein would bear the ectopic 6O-sulfated HS presented by the hypodermis that misdirects the DB7 motor neuron. To this end, we systematically removed the genes coding for four canonical HS core proteins in the *C. elegans* genome, *lon-2*/glypican, *gpn-1*/glypican, *sdn-1*/syndecan, or *unc-52*/perlecan, respectively, and tested the effect on DB7 motor neuron projection patterns in animals expressing *hst-6* in the hypodermis. We find that removal of *lon-2*/glypican but none of the other HS core proteins suppresses the axonal misrouting of DB7 to a level that is statistically indistinguishable from wild-type (Figure 3E). As *lon-2*/glypican normally acts in the hypodermis [10], our data suggest that the ectopic HS structures in the hypodermis that redirect DB7 may be attached to the LON-2/glypican HS core protein.

We next sought to address how alterations in HS-modification patterns exert an impact on the DB7 motor axon guidance decision. HS may play a role in determining ligand/receptor binding specificities in vitro (reviewed in [3]), so we reasoned that changing HS-modification patterns may reprogram the responsiveness of motor axons to defined cues. To address this possibility, we asked whether a specific axon guidance cue is required for the misrouting of individual motor axons induced by ectopic 6O-sulfation. The guidance cue *slt-1*/Slit is known to require different HS modifications in distinct cellular contexts in *C. elegans* [7]. *Slit*-mediated axon growth at the fly midline, and in vertebrate tissue explants, are also known to require the presence of HS, albeit of unknown modification status [16–18]. The ligand *slt-1*/Slit signals through *sax-3*/Robo of the Robo family of guidance receptors [19]. More recently, EVA-1, a conserved transmembrane protein with extracellular domains that display similarity to sugar binding domains, has been identified as an additional Slit/SLT-1 receptor that is required for Slit/SLT-1 signaling and physically interacts with SLT-1 [20].

DA/DB motor neurons and in particular DB7 do not require *slt-1* or *eva-1* to make their correct guidance decision at the midline while its canonical receptor *sax-3*/Robo is involved in routing all DA/DB motor neurons (Figure 3D; Figure S1B). These findings are consistent with previous findings demonstrating that *sax-3*/Robo has functions that are independent of its canonical ligand *slt-1*/Slit [7, 19] and imply that this *slt-1*-independent function of *sax-3*/Robo is likewise independent of *eva-1*. Intriguingly, loss of *slt-1* significantly suppresses the axonal projection defects in DB7 as a result of ectopically expressing *hst-6* in the hypodermis (Figure 3F). This suppression does not result from changes in expression levels of either *slt-1* or its canonical receptor *sax-3* (Figure S5). Thus, a possible interpretation of our data is that ectopic 6O-sulfated HS attached to LON-2/glypican instructs SLT-1 to misroute the DB7 motor axon by possibly promoting the interaction of SLT-1 with a cognate receptor on motor neurons, thereby misrouting an extending axon.

We next asked whether the *slt*-1/Slit receptor *eva-1* could serve as this cognate receptor in the context of DB7 misrouting. Indeed, genetic removal of *eva-1* significantly suppresses the *hst-6*-dependent axonal misrouting of DB7 (Figure 3F). With *eva-1* expressed in eMNs [20], this genetic data is in accord with a scenario where HS of a specific modification status instructs *slt-1* to interact with *eva-1*, leading to an axonal misrouting response of DB7. The misrouting of DB7 must be largely *sax-3* independent because the penetrance of defects in the *hst-6* misexpression strain (10.2%) and *sax-3* loss-of-function animals (19.8%) are additive in the strain carrying the *hst-6*-misexpressing transgene in conjunction with the *sax-3* null mutation (34.3%) (compare Figures 3D and 3F). This last finding implies potential *sax-3*-independent functions for *eva-1.*

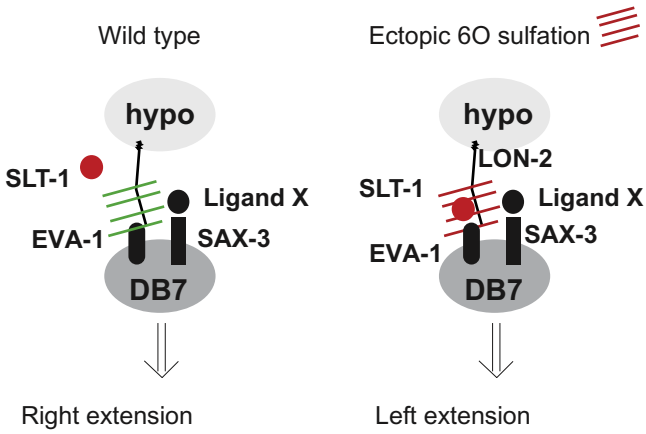


Figure 4. A Model for the Role of HS in Redirecting Axonal Projections

A possible interpretation of the genetic data presented in Figure 3. In wild-type animals, *slt-1* or *eva-1* is not required for DB7 neuron projections (as *slt-1* and *eva-1* mutants show no axonal defects; Figure 3D), whereas *sax-3* does normally have a role in DB7 axon extension (Figure 3D). In wild-type animals, SAX-3 may therefore be interacting with an as yet unknown ligand X. Upon introducing ectopic 6O-sulfation patterns (red hatches), an interaction of the SLT-1 protein with EVA-1 may be promoted, which supersedes the effect normally induced by SAX-3/Ligand X. We emphasize that these conclusions are based on purely genetic arguments and that more indirect mechanistic models can be envisioned that are not shown here.

## Discussion

Our analysis of the projection patterns of embryonic motor axons in *C. elegans* reveals that superficially similar neuron types are programmed to extend their axons in distinct directions through diverse mechanisms. In addition to a large number of guidance cues and intracellular signaling molecules, which are involved in patterning motor axon projections at the worm midline (data not shown), HS modifications play a crucial role in determining the projection patterns of individual motor axons. Our findings indicate that HS modifications have specific and instructive functions, likely through mediating specific ligand/receptor interactions (Figure 4).

This interpretation takes the broadly accepted concept into account that extracellular HS molecules not only promote, but are often essential for, the activity of specific ligand/receptor systems [3]. In support of this notion, in vitro experiments suggest that differentially modified HS can promote signaling through distinct signaling systems [21, 22]. Together with our finding that both the removal of enzymes that modify HS molecules as well as the ectopic addition of HS modifications through misexpression of a HS-modifying enzyme causes misrouting defects, we propose that the local modification status of HS in the vicinity of extending motor axons impinges on which ligand/receptor system is engaged (Figure 4). This model is consistent not only with the effects observed upon removal of HS-modifying enzymes, but also with the genetic analyses of animals with ectopic expression of *hst-6* in the hypodermis. In this scenario, the introduction of a novel HS-modification pattern that is attached to a specific core protein in the hypodermis (LON-2) aberrantly promotes the interaction of the repulsive SLT-1 cue with a receptor molecule, possibly EVA-1, thereby causing a misorientation of motor axon pathfinding (Figure 4). This is supported by our genetic data demonstrating that genetic removal of *lon-2*, *slt-1*, or *eva-1* suppresses the misrouting defect in DB7 to levels that are statistically indistinguishable from wild-type (Figures 3D–3F). However, we note that this model is not the only way to interpret the genetic interaction of ectopic *hst-6* with *lon*-2, *slt-1*, or *eva-1.* Indirect effects are conceivable and can not be ruled out by genetic analysis alone.

With this caveat in mind, the finding that ectopic expression of an HS-modifying enzyme and the dependence of the resulting phenotype on a specific axon-guidance molecule (*slt-1*) and one of its receptors (*eva-1*) provides additional support for a concept in which the enormous molecular complexity embedded with HS molecules may carry not merely permissive but also instructive information content. It has been speculated before that the molecular diversity of HS molecules could provide a code that regulates the regiospecific activity of individual axon-patterning systems [3, 5–7]. Specifically, in the HS code hypothesis, regiospecific HS-modification patterns determine the responsiveness of neurons to individual ligand/receptor patterning cues. In accordance with this hypothesis, the removal of individual modifications causes highly specific nervous system-patterning defects [7, 23–25] (this study). Furthermore, we show that the removal of combinations of HS modifications uncovers cell-specific redundancies in the requirements for HS modifications (Figure 2), indicating that the presumptive HS code may be degenerate. And lastly, as pointed out previously [13], an important additional criterion for the existence of such a code is that HS modifications act instructively, and not merely as permissive cofactors. A genetic test to determine the difference between instructiveness and permissiveness is to ask whether a given gene not only

displays a specific loss-of-function phenotype, but whether a gain-of-function phenotype of the gene upon misexpression can also instruct a novel phenotype [26]. Keeping in mind that these experiments provide genetic rather than biochemical evidence for the action of HS, our results clearly show that we can redirect the DB7 neuron upon misexpression of the HS 6O-sulfotransferase *hst-6*. We can detect the molecular correlate of this *hst-6* misexpression in the hypodermis by using both an HS-specific antibody and biochemical analyses of HS disaccharides (Figure 2B; Figure S2). Moreover, we find that this novel phenotype is dependent on a specific HS core protein (*lon-2*/glypican) and that aberrant 6O-sulfation appears to activate *slt-1* signaling through the *slt-1* receptor *eva-1* (Figures 3E and 3F). Further biochemical studies are warranted to corroborate these genetic results and to gain mechanistic insight into how HS can misdirect axons.

## Experimental Procedures

### Neuroanatomical Scoring

All animals were scored at 20°C in a mixed population of midlarval to adult stages. DA/DB were scored with *unc-129::gfp (evIs82b)* and PVQ with *sra-6::gfp (oyIs14).* GFP expression in the DA/DB neurons of *evIs82b* transgenic animals is variable in DA7, DA8, and DA9; moreover, projection patterns of DA1, DB1, and DB2 are often not easy to follow on the single-cell level and we therefore excluded these neuron types from our analysis. Individual motor neurons were identified based on their cell-body position and the dorsal projection patterns. In each figure, the error bars denote the standard error of proportion and asterisks indicate statistical significance: *$p < 0.05$, **$p < 0.005$, ***$p < 0.0005$; n.s., not significant. Statistical significance was calculated with the z-test. If multiple comparisons were made, p values were subjected to the Bonferroni correction.

### Transgenes

For ectopic hypodermal expression of HS-modifying enzymes, the complete *hst-6* and *hst-2* loci were fused to the *dpy-7* promoter [14] by PCR fusion [27]. For the *dpy-7$^{prom}$::hst-6$^{mut}$* construct, the template for PCR fusion was genomic DNA from OH281 [*mgIs18*; *lon-2(e678)hst-6(ot17)*], which harbors a premature stop codon in *hst-6* [28]. All constructs were injected at 2.5 ng/μl into *evIs82b* (*Is[unc-129::gfp]*) with *pceh-22::gfp* at 50 ng/μl as injection marker and *pBS* at 50 ng/μl as carrier.

### Immunohistochemistry

Worms were prepared for immunohistochemistry with a freeze crack protocol [29] followed by 20 min fixations in ice-cold acetone and methanol, respectively. Worms were then incubated for 30 min in PBS containing 10% donkey serum and in the same buffer at 4°C overnight with antibody AO4B08 or HS4C3 (1:5) [15, 30]. The immunohistochemical stain was developed with the monoclonal anti-VSV antibody P5D4 (dilution 1:250) and Alexa-labeled (555) donkey anti-mouse antibodies (dilution 1:250).

### Supplemental Data

Supplemental Data include five figures and two tables and can be found with this article online at http://www.current-biology.com/supplemental/S0960-9822(08)01538-8.

### Acknowledgments

We thank Q. Chen and M. Attreed for expert technical assistance; the CGC, D. Sherwood, J. Culotti, Y. Jin, C. Bargmann, and C. Li for providing strains; D. Hall and R. Durbin for providing embryonic electron micrographs; R. Freemont for initial antibody stains; A. Boyanov for EM image analysis; and several colleagues, J. Culotti, and members of the Hobert and Bülow labs for comments on the manuscript. This work was funded in part by the Muscle Dystrophy Association, by the McKnight Foundation, and by NIH grants 2R01NS039996-05 and 5R01NS050266-03 to O.H., 5R01HD055380 to H.E.B., and 5T32NS07098 to R.A.T. H.E.B. is an Alfred P. Sloan Fellow. O.H. is an Investigator of the HHMI.

Received: January 22, 2008
Revised: October 28, 2008
Accepted: November 10, 2008
Published online: December 4, 2008

### References

1. Lee, J.S., and Chien, C.B. (2004). When sugars guide axons: insights from heparan sulphate proteoglycan mutants. Nat. Rev. Genet. *5*, 923–935.
2. Van Vactor, D., Wall, D.P., and Johnson, K.G. (2006). Heparan sulfate proteoglycans and the emergence of neuronal connectivity. Curr. Opin. Neurobiol. *16*, 40–51.
3. Bülow, H.E., and Hobert, O. (2006). The molecular diversity of glycosaminoglycans shapes animal development. Annu. Rev. Cell Dev. Biol. *22*, 375–407.
4. Esko, J.D., and Selleck, S.B. (2002). Order out of chaos: assembly of ligand binding sites in heparan sulfate. Annu. Rev. Biochem. *71*, 435–471.
5. Turnbull, J., Powell, A., and Guimond, S. (2001). Heparan sulfate: decoding a dynamic multifunctional cell regulator. Trends Cell Biol. *11*, 75–82.
6. Park, P.W., Reizes, O., and Bernfield, M. (2000). Cell surface heparan sulfate proteoglycans: selective regulators of ligand-receptor encounters. J. Biol. Chem. *275*, 29923–29926.
7. Bülow, H.E., and Hobert, O. (2004). Differential sulfations and epimerization define heparan sulfate specificity in nervous system development. Neuron *41*, 723–736.
8. Kramer, K.L., and Yost, H.J. (2002). Ectodermal syndecan-2 mediates left-right axis formation in migrating mesoderm as a cell-nonautonomous Vg1 cofactor. Dev. Cell *2*, 115–124.
9. Hudson, M.L., Kinnunen, T., Cinar, H.N., and Chisholm, A.D. (2006). *C. elegans* Kallmann syndrome protein KAL-1 interacts with syndecan and glypican to regulate neuronal cell migrations. Dev. Biol. *294*, 352–365.
10. Gumienny, T.L., MacNeil, L.T., Wang, H., de Bono, M., Wrana, J.L., and Padgett, R.W. (2007). Glypican LON-2 is a conserved negative regulator of BMP-like signaling in *Caenorhabditis elegans*. Curr. Biol. *17*, 159–164.
11. Rogalski, T.M., Williams, B.D., Mullen, G.P., and Moerman, D.G. (1993). Products of the *unc-52* gene in *Caenorhabditis elegans* are homologous to the core protein of the mammalian basement membrane heparan sulfate proteoglycan. Genes Dev. *7*, 1471–1484.
12. Ackley, B.D., Kang, S.H., Crew, J.R., Suh, C., Jin, Y., and Kramer, J.M. (2003). The basement membrane components nidogen and type XVIII collagen regulate organization of neuromuscular junctions in *Caenorhabditis elegans*. J. Neurosci. *23*, 3577–3587.
13. Holt, C.E., and Dickson, B.J. (2005). Sugar codes for axons? Neuron *46*, 169–172.
14. Gilleard, J.S., Barry, J.D., and Johnstone, I.L. (1997). *cis* regulatory requirements for hypodermal cell-specific expression of the *Caenorhabditis elegans* cuticle collagen gene *dpy-7*. Mol. Cell. Biol. *17*, 2301–2311.
15. Kurup, S., Wijnhoven, T.J., Jenniskens, G.J., Kimata, K., Habuchi, H., Li, J.P., Lindahl, U., van Kuppevelt, T.H., and Spillmann, D. (2007). Characterization of anti-heparan sulfate phage display antibodies AO4B08 and HS4E4. J. Biol. Chem. *282*, 21032–21042.
16. Johnson, K.G., Ghose, A., Epstein, E., Lincecum, J., O'Connor, M.B., and Van Vactor, D. (2004). Axonal heparan sulfate proteoglycans regulate the distribution and efficiency of the repellent slit during midline axon guidance. Curr. Biol. *14*, 499–504.
17. Steigemann, P., Molitor, A., Fellert, S., Jackle, H., and Vorbruggen, G. (2004). Heparan sulfate proteoglycan syndecan promotes axonal and myotube guidance by slit/robo signaling. Curr. Biol. *14*, 225–230.
18. Hu, H. (2001). Cell-surface heparan sulfate is involved in the repulsive guidance activities of Slit2 protein. Nat. Neurosci. *4*, 695–701.
19. Hao, J.C., Yu, T.W., Fujisawa, K., Culotti, J.G., Gengyo-Ando, K., Mitani, S., Moulder, G., Barstead, R., Tessier-Lavigne, M., and Bargmann, C.I. (2001). *C. elegans* Slit acts in midline, dorsal-ventral, and anterior-posterior guidance via the SAX-3/Robo receptor. Neuron *32*, 25–38.
20. Fujisawa, K., Wrana, J.L., and Culotti, J.G. (2007). The slit receptor EVA-1 coactivates a SAX-3/Robo mediated guidance signal in *C. elegans*. Science *317*, 1934–1938.
21. Guimond, S.E., and Turnbull, J.E. (1999). Fibroblast growth factor receptor signalling is dictated by specific heparan sulphate saccharides. Curr. Biol. *9*, 1343–1346.

22. Irie, A., Yates, E.A., Turnbull, J.E., and Holt, C.E. (2002). Specific heparan sulfate structures involved in retinal axon targeting. Development *129*, 61–70.
23. Kinnunen, T., Huang, Z., Townsend, J., Gatdula, M.M., Brown, J.R., Esko, J.D., and Turnbull, J.E. (2005). Heparan 2-O-sulfotransferase, *hst-2*, is essential for normal cell migration in *Caenorhabditis elegans*. Proc. Natl. Acad. Sci. USA *102*, 1507–1512.
24. Pratt, T., Conway, C.D., Tian, N.M., Price, D.J., and Mason, J.O. (2006). Heparan sulphation patterns generated by specific heparan sulfotransferase enzymes direct distinct aspects of retinal axon guidance at the optic chiasm. J. Neurosci. *26*, 6911–6923.
25. McLaughlin, D., Karlsson, F., Tian, N., Pratt, T., Bullock, S.L., Wilson, V.A., Price, D.J., and Mason, J.O. (2003). Specific modification of heparan sulphate is required for normal cerebral cortical development. Mech. Dev. *120*, 1481–1488.
26. Held, L.I. (2002). Imaginal Discs: The Genetic and Cellular Logic of Pattern Formation (Cambridge, UK: Cambridge University Press).
27. Hobert, O. (2002). PCR fusion-based approach to create reporter gene constructs for expression analysis in transgenic *C. elegans*. Biotechniques *32*, 728–730.
28. Bülow, H.E., Berry, K.L., Topper, L.H., Peles, E., and Hobert, O. (2002). Heparan sulfate proteoglycan-dependent induction of axon branching and axon misrouting by the Kallmann syndrome gene *kal-1*. Proc. Natl. Acad. Sci. USA *99*, 6346–6351.
29. Duerr, J.S. (2006). Immunohistochemistry. In Wormbook, The *C. elegans* Research Community, ed. doi/10.1895/wormbook.1.105.1, http://www.wormbook.org.
30. Ten Dam, G.B., Kurup, S., van de Westerlo, E.M., Versteeg, E.M., Lindahl, U., Spillmann, D., and van Kuppevelt, T.H. (2006). 3-O-sulfated oligosaccharide structures are recognized by anti-heparan sulfate antibody HS4C3. J. Biol. Chem. *281*, 4654–4662.
31. Rhiner, C., Gysi, S., Fröhli, E., Hengartner, M.O., and Hajnal, A. (2005). Syndecan regulates cell migration and axon guidance in *C. elegans*. Development *132*, 4621–4633.
32. Durbin, R.M. (1987). Studies on the development and organisation of the nervous system of *Caenorhabditis elegans*. PhD thesis, University of Cambridge, Cambridge, UK.
33. Sherwood, D.R., Butler, J.A., Kramer, J.M., and Sternberg, P.W. (2005). FOS-1 promotes basement-membrane removal during anchor-cell invasion in *C. elegans*. Cell *121*, 951–962.